EPJ Web of Conferences **71**, 00034 (2014)
DOI: 10.1051/epjconf/20147100034

New ATLAS results in SUSY searches for 3rd generation squarks and electroweak production

Claire David (on behalf of the ATLAS Collaboration)[1,a]

[1] *University of Victoria*

Abstract. Naturalness arguments for weak-scale supersymmetry favour supersymmetric partners of the third generation quarks with masses close to those of their Standard Model counterparts. Real and virtual production of third generation squarks via decay of a gluino can be significant if the mass of the gluino does not exceed the TeV scale. Top or bottom squarks with masses less than a few hundred GeV can also give rise to direct pair production rates at the LHC that can be observed in the 8 TeV data sample recorded by the ATLAS detector. Moreover, many supersymmetric models feature neutralinos, charginos and even sleptons with masses less than a few hundred GeV so that they can be observed in the available data sample. The talk presents recent ATLAS results from searches for direct stop and sbottom pair production as well as pair production of charginos, neutralinos and sleptons.

1 Introduction

1.1 Motivations

The Standard Model (SM) of particles and fields describes experimental data over a large energy range and many of its predictions have been succesfully tested at the per mille level. The SM is however considered as a low energy effective theory as the scalar sector is unstable under radiative corrections and new phenomena are expected at the TeV scale.

Supersymmetry[1] (SUSY) provides an extension of the Standard Model (SM) that solves the hierarchy problem by introducing supersymmetric partners of the known bosons and fermions. In the framework of the *R*-parity-conserving minimal supersymmetric extension of the SM (MSSM), SUSY particles are produced in pairs and the lightest supersymmetric particle (LSP) is stable, providing a possible candidate for dark matter.

In a large variety of models, the LSP is the lightest neutralino ($\tilde{\chi}_1^0$). The coloured superpartners of quarks and gluons, the squarks ($\tilde{q}$) and the gluinos ($\tilde{g}$), if not too heavy, would be produced in strong interaction processes at the Large Hadron Collider (LHC) and decay via cascades ending with the LSP. The undetected LSP would result in missing transverse momentum ($E_{\mathrm{T}}^{\mathrm{miss}}$) while the rest of the cascade would yield final states with multiple jets and possibly leptons. A study of the expected SUSY particle spectrum derived from naturalness considerations suggests that the supersymmetric

[a] e-mail: claire.david@cern.ch
[1] Theoretical references can be found in the respective experimental works cited.

partners of the third-generation SM quarks are the lightest coloured supersymmetric particles. This may lead to the lightest bottom squark (sbottom, $\tilde{b}_1$) and top squark (stop, $\tilde{t}_1$) mass eigenstates being significantly lighter than the other squarks and the gluinos. As a consequence, $\tilde{b}_1$ and $\tilde{t}_1$ could be pair-produced with relatively large cross sections at the LHC.

If the masses of the gluinos and squarks are large, the direct production of charginos, neutralinos and sleptons may dominate the production of SUSY particles at the LHC. Such a scenario is possible in the general framework of the phenomenological minimal supersymmetric SM (pMSSM). Naturalness suggests that third-generation sparticles, charginos and neutralinos should have masses of a few hundreds of GeV. Light sleptons are expected in gauge-mediated and anomaly-mediated SUSY breaking scenarios. Light sleptons could also play a role in the co-annihilation of neutralinos, leading to a dark matter relic density consistent with cosmological observations.

Here, the focus will be on the latests results using more than 20.1 fb^{-1} of proton-proton collisions at $\sqrt{s} = 8$ TeV with the ATLAS [1] experiment at the LHC.

1.2 The ATLAS detector

The analyses described in this review collectively make use of all the detector systems that constitute the ATLAS detector. The inner detector, used to reconstruct charged particle tracks and vertices, consists of silicon pixels, silicon strips and transition radiation detectors, covering $|\eta| < 2.5$ in in pseudorapidity[2]. It is immersed in a homogeneous solenoidal magnetic field, which allows to measure the momentum of charged particles using track curvature. The calorimeters, responsible for the reconstruction of particle showers, are made of liquid argon and lead in the electromagnetic part, while the hadronic part is composed of scintillating tiles and iron in the central region and liquid argon, copper and tungsten in the forward region. Outside the calorimeter, toroid magnets provide the field for the muon spectrometer, which consists of resistive-plate and thin-gap trigger chambers, and three sets of drift tubes and cathode strip chambers allowing for the reconstruction of muon tracks with high precision.

2 Direct production of 3rd generation squarks

2.1 Direct sbottom production decaying to neutralino 1

The analysis presented in Ref. [2] uses 20.1 fb^{-1} of pp collisions at $\sqrt{s} = 8$ TeV collected by the ATLAS detector. It considers a SUSY mass spectrum where the lightest sbottom is the only coloured sparticle contributing to the production processes and it only decays via $\tilde{b}_1 \rightarrow b\tilde{\chi}_1^0$. This results in the production of jets of particles with high transverse momentum (p_{T}). Jets in ATLAS are reconstructed from three-dimensional cell-energy clusters in the calorimeter using the anti-k_t jet algorithm [3] with a radius parameter of 0.4. In this analysis, events are characterised by the presence of two jets originating from the hadronisation of the b-quarks (b-tagged) and large missing transverse momentum. The contransverse mass m_{CT} [4] is a kinematic variable that can be used to measure the masses of pair-produced semi-invisibly decaying heavy particles. For two identical decays of heavy particles into two visible particles (or particle aggregates) v_1 and v_2, and two invisible particles, m_{CT} is defined as: $m_{\mathrm{CT}}^2(v_1, v_2) = [E_{\mathrm{T}}(v_1) + E_{\mathrm{T}}(v_2)]^2 - [\mathbf{p}_{\mathrm{T}}(v_1) - \mathbf{p}_{\mathrm{T}}(v_2)]^2$, where $E_T = \sqrt{p_{\mathrm{T}}^2 + m^2}$. In this analysis, v_1 and v_2 are the two b-jets from the squark decays and the invisible particles are the two neutralinos. This variable has kinematic endpoints, in particular an upper bound for sbottom production correlated to the mass difference squared between sbottom and $\tilde{\chi}_1^0$.

[2]Pseudorapidity is defined in terms of the polar angle θ as $\eta = -\ln\tan(\theta/2)$, while ϕ is the azimuthal angle.

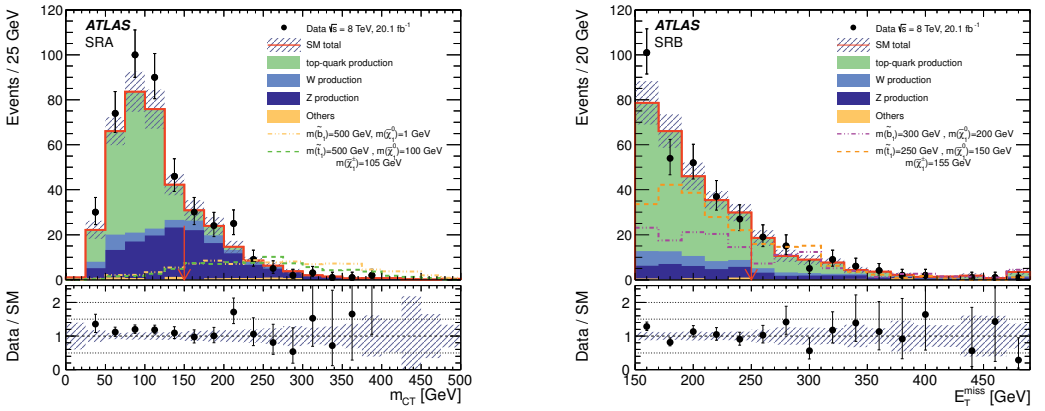

Figure 1: Distribution of m_{CT} in SRA (left) with all the selection criteria applied except the m_{CT} thresholds and $E_{\mathrm{T}}^{\mathrm{miss}}$ in SRB (right) with all SRB selection criteria applied except the final $E_{\mathrm{T}}^{\mathrm{miss}}$ requirement. The shaded band includes statistical, detector-related and theoretical systematic uncertainties. The backgrounds are normalised to the values determined in the fit. The red arrow indicates where a selection on the corresponding variable is applied. For illustration the distributions expected for two signal models are displayed. For SRB (right), the tested model here correspond to $m_{\tilde{b}_1} = 300$ GeV and $m_{\tilde{\chi}_1^0} = 200$ GeV (purple dash-dot line). The rightmost bin includes the overflows. [2]

Two sets of signal regions are defined to provide sensitivity to the kinematic topologies associated with different mass splittings between the sbottom and the neutralino. Signal region A (SRA) targets signal events with large mass splitting between the squark and the neutralino, identifying two high-p_{T} leading b-tagged jets as products of the two sbottom decays. Additional requirements based on other kinematic variables aim at suppressing the multijets background, as well as contributions from production of top-quark and Z-bosons in association with heavy-flavour jets. Signal region B (SRB) is defined to enhance the sensitivity for a small squark–neutralino mass difference, where the b-quarks may have transverse momenta below the reconstruction thresholds applied in the analysis. In this compressed scenario, events are explicitly selected with a high-p_{T} jet (not b-tagged). This leading jet is likely to have been produced as initial-state radiation (ISR) and recoils against the squark pair system. The contransverse mass distribution of SRA events and the transverse missing momentum spectrum of SRB events are shown in Figure 1. No significant excess above the SM expectation is observed in any of the signal regions. Limits at 95% CL are set, excluding sbottom masses up to 620 GeV for $m_{\tilde{\chi}_1^0}$ <120 GeV (520 GeV if the branching ratio (BR) of $\tilde{b}_1 \rightarrow b + \tilde{\chi}_1^0$ is reduced to 60%, for $m_{\tilde{\chi}_1^0}$ <150 GeV). Differences in mass above 50 GeV between the $\tilde{b}_1$and the $\tilde{\chi}_1^0$ are excluded up to sbottom masses of 300 GeV. Figure 2 shows the observed (solid lines) and expected (dashed lines) exclusion limits for the sbottom pair production scenario.

2.2 Direct sbottom production decaying to neutralino 2

This analysis presented in [5] addresses a model in which the $\tilde{b}_1$ is produced in pairs and decays exclusively via $\tilde{b}_1 \rightarrow b + \tilde{\chi}_2^0$. The mass of the LSP neutralino $\tilde{\chi}_1^0$ is set to 60 GeV. Only the configuration $m_{\tilde{\chi}_2^0} > m_{\tilde{\chi}_1^0} + m_h$ is studied, where the decay $\tilde{\chi}_2^0 \rightarrow h + \tilde{\chi}_1^0$ has 100% branching ratio. Signal events

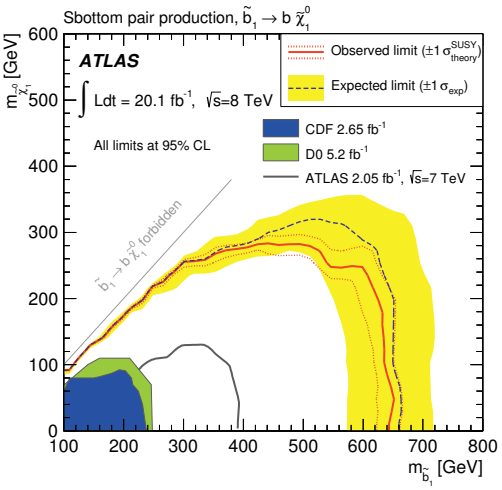

Figure 2: Expected and observed exclusion limits at 95% CL in the $(m_{\tilde{b}_1}, m_{\tilde{\chi}_1^0})$ mass plane for the sbottom pair production scenario considered. The signal region providing the best expected CLs exclusion limit is chosen at each point. The dashed (solid) lines show the expected (observed) limits, including all uncertainties except for the theoretical signal cross-section uncertainty (PDF and scale). The bands around the expected limits show the $\pm 1\,\sigma$ uncertainties. The dotted lines around the observed limits represent the results obtained when moving the nominal signal cross section up or down by the $\pm 1\,\sigma$ theoretical uncertainty. [2]

considered here are both Higgs bosons decay into a $b\bar{b}$ pair, yielding a signature with no lepton, six bottom quarks and large $E_{\mathrm{T}}^{\mathrm{miss}}$. The jets and tagged b-jets should pass several selection criteria. The events are further classified in various "signal regions", each defined by a set of selection criteria that make use of several variables calculated from the reconstructed objects.

The main source of reducible background is the production of $t\bar{t}$ events in association with additional non-b jets, where a c-jet or a τ-lepton decaying to hadrons and a ν_τ is mistagged as a b-jet. All reducible background sources are estimated simultaneously using a data-driven method that predicts the contribution from events with at least one mistagged b-jet. This estimate is based on a matrix method (MM). As a validation, a "closure" test is performed by applying the method directly on the $t\bar{t}$ Monte Carlo (MC) simulation.

The results are in agreement with the SM background predictions and translate into 95% CL upper limits. Sbottom masses between 320 and 600 GeV are excluded for $m_{\tilde{\chi}_2^0} = 300$ GeV. No exclusion limits are obtained for low $m_{\tilde{\chi}_2^0}$ due to the presence of soft b-jets in the final states. The sensitivity of this analysis to $\tilde{b}_1$ pair production processes where $\tilde{b}_1 \to b + \tilde{\chi}_2^0, \tilde{\chi}_2^0 \to h + \tilde{\chi}_1^0$, depends on $m_{\tilde{\chi}_2^0}$. For higher neutralino masses, the sensitivity decreases because of the tight $E_{\mathrm{T}}^{\mathrm{miss}}$ and the jets p_{T} thresholds. The $E_{\mathrm{T}}^{\mathrm{miss}}$ distribution obtained using 20.1 fb^{-1} of pp collisions taken in 2012 at $\sqrt{s} = 8$ TeV and the expected and observed exclusion limits for the direct sbottom scenario are shown on Figure 3.

2.3 Direct stop production decaying to bottom and top

The stop can decay into a variety of final states, depending, amongst other factors, on the mass hierarchy of the lightest chargino and the lightest neutralino. Two decay modes are considered separately in Ref. [6], each assumed to have 100% branching ratio: $\tilde{t}_1 \to b + \tilde{\chi}_1^{\pm}$, and $\tilde{t}_1 \to t + \tilde{\chi}_1^0$. The first decay mode requires $m_{\tilde{t}_1} - m_{\tilde{\chi}_1^{\pm}} > m_b$, the $\tilde{\chi}_1^{\pm}$ subsequently decaying into the lightest neutralino (assumed to be the LSP), and a real or virtual W boson. In the second decay mode, only on-shell top quarks are considered, limiting the analysis to a stop heavier than the top quark and the lightest neutralino. In both cases the stops are pair-produced. Events are characterised by the presence of two isolated leptons (e, μ) with opposite charge, two b-quarks and significant transverse momentum. Good sensitivity is reached by exploiting the different bounds of the stransverse mass, defined as

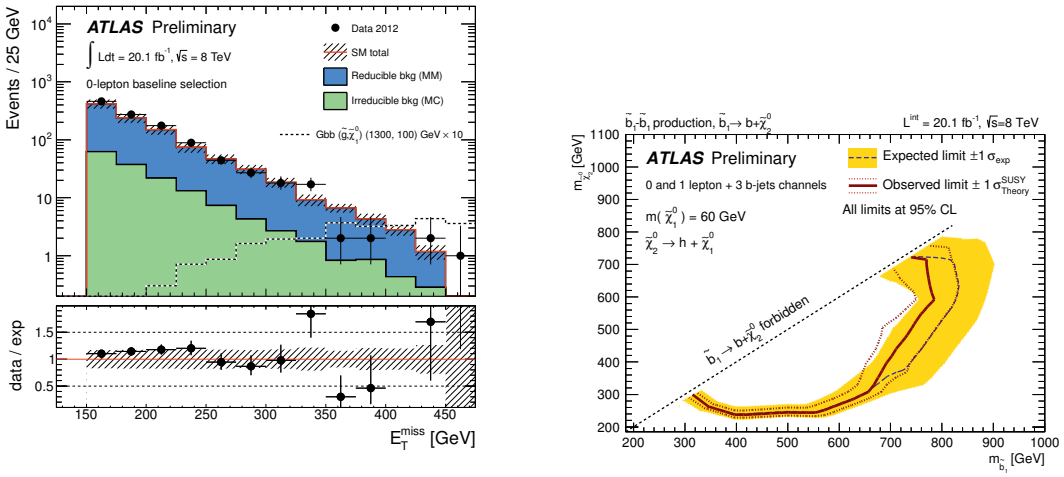

Figure 3: The $E_{\mathrm{T}}^{\mathrm{miss}}$ distribution (left) observed in data after the baseline selection and the requirement of at least 4 jets with p_{T}> 30 GeV, together with the background prediction. The prediction from the matrix method for the reducible background (MM) is shown in blue and the irreducible background from MC is shown in green. The ratio between the observed event yield and background prediction is also shown. The shaded bands include all systematic uncertainties on the MC and the matrix method predictions. Exclusion limits (right) in the ($m_{\tilde{b}_1}$,$m_{\tilde{\chi}_2^0}$) plane for the direct sbottom model. [5]

$m_{\mathrm{T2}}(\mathbf{p}_{\mathrm{T}}^1, \mathbf{p}_{\mathrm{T}}^2, \mathbf{q}_{\mathrm{T}}) = \min_{\mathbf{q}_{\mathrm{T}}^1+\mathbf{q}_{\mathrm{T}}^2=\mathbf{q}_{\mathrm{T}}} \left\{\max[\, m_{\mathrm{T}}(\mathbf{p}_{\mathrm{T}}^1, \mathbf{q}_{\mathrm{T}}^1), m_{\mathrm{T}}(\mathbf{p}_{\mathrm{T}}^2, \mathbf{q}_{\mathrm{T}}^2)\,]\right\}$, where $\mathbf{p}_{\mathrm{T}}^1$ and $\mathbf{p}_{\mathrm{T}}^2$ are the transverse momenta of two particles and the transverse mass is $m_T = \sqrt{2|\mathbf{p}_{\mathrm{T}}^1||\mathbf{p}_{\mathrm{T}}^2|(1-\cos\phi)}$ (ϕ is the angle between the particles with transverse momenta $\mathbf{p}_{\mathrm{T}}^1$ and $\mathbf{p}_{\mathrm{T}}^2$ in the transverse plane). The minimisation is performed over all the possible decompositions of $\mathbf{q}_{\mathrm{T}}$. For $t\bar{t}$ and WW production, this variable computed with two lepton transverse momenta and the transverse missing momentum ($m_{\mathrm{T2}}(\ell, \ell, E_{\mathrm{T}}^{\mathrm{miss}})$) is bound sharply from above by the mass of the W. For $t\bar{t}$ production, the variable computed using the two b-jets ($m_{\mathrm{T2}}^{\text{b-jet}}(b, b, \ell + \ell + E_{\mathrm{T}}^{\mathrm{miss}})$) has a kinematic end-point correlated to the squared difference between the mass of the top and of the W, whilst for stop decays the bound is strongly correlated to the mass difference between the stop and the chargino. A high cut on this variable is thus sensitive to large stop-chargino mass differences and small chargino-neutralino mass differences. Figure 4 shows the $m_{\mathrm{T2}}^{\text{b-jet}}$ distribution for the $\tilde{t}_1 \rightarrow b + \tilde{\chi}_1^{\pm}$ decay mode, obtained using 20.3 fb^{-1} of data taken at $\sqrt{s} = 8$ TeV.

In the $\tilde{t}_1 \rightarrow t + \tilde{\chi}_1^0$ search, signal events are separated from SM backgrounds using a multivariate analysis (MVA) technique based on boosted decision trees (BDT). Discriminating variables are used as input to a gradient boosting algorithm (BDTG), where the $m_{\mathrm{T2}}^{\text{b-jet}}$ variable is one of the most effective inputs. Figure 5 shows the BDTG spectrum. No excess is observed. The results are used to derive limits at 95% CL on the masses of the $\tilde{\chi}_1^{\pm}$ and $\tilde{\chi}_1^0$ for a stop of 300 GeV mass which is pair-produced and decays with 100% BR into a chargino and a b-quark. Figure 6 shows the combined exclusion limits with previous searches [8].

Figure 7 shows the exclusion limits for the $\tilde{t}_1 \rightarrow t + \tilde{\chi}_1^0$ scenario. A supersymmetric top squark of mass between 220 GeV and 520 GeV decaying with 100% BR to a t-quark and the lightest neutralino is excluded at 95% CL for a massless neutralino.

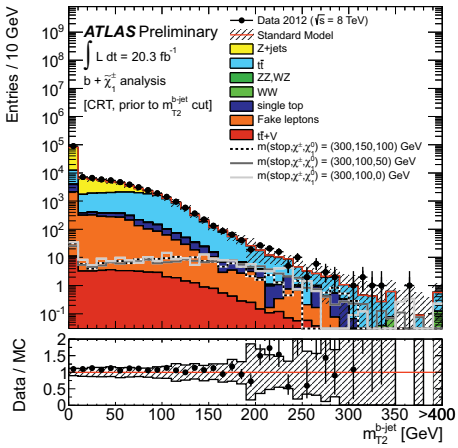

Figure 4: Distribution of $m_{\mathrm{T2}}^{\text{b-jet}}$ after all SR requirements, except that on $m_{\mathrm{T2}}^{\text{b-jet}}$ itself. The contributions from all SM backgrounds are shown; the bands represent the total uncertainty. The component labelled "fake lepton" is estimated from data and the component labelled $t\bar{t}$ is shown re-normalised after the background fit. [6]

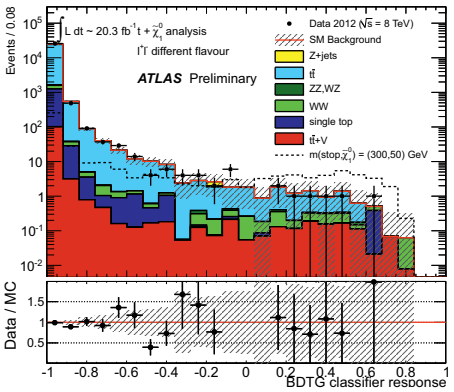

Figure 5: BDTG distribution in the $t + \tilde{\chi}_1^0$ analysis after all selection requirements, except the cut on the BDTG itself, after the background fit and for the different flavour lepton pair (top) and same flavour lepton pair (bottom) channels, as obtained from the trainings which used the point $(m(\tilde{t}), m(\tilde{\chi}_1^0))$=(300,50) GeV and $(m(\tilde{t}), m(\tilde{\chi}_1^0))$=(300,100) GeV, respectively. The reference signal points used in the training of each channel are also shown. [6]

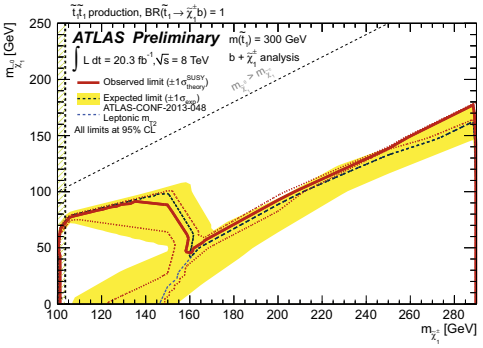

Figure 6: Exclusion limits at 95% CL from the analysis of 20.3 fb^{-1} of 8 TeV collision data on the masses of the chargino and the lightest neutralino, for a stop with a mass of 300 GeV and assuming BR($\tilde{t}_1 \to b + \tilde{\chi}_1^{\pm}$) = 1. [6]

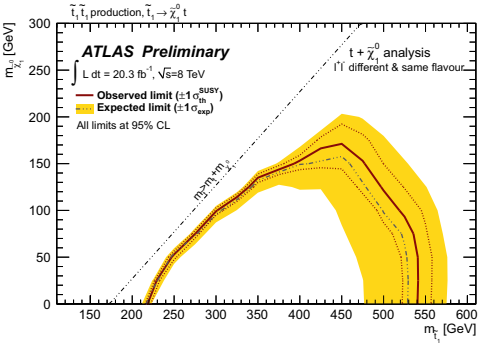

Figure 7: t+$\tilde{\chi}_1^0$ analysis: exclusion limits at 95% CL in the $m(\tilde{t}_1) - m(\tilde{\chi}_1^0)$ plane for the combination of the same flavour and different flavour channel from the analysis of 20.3 fb^{-1} of 8 TeV collision data. [6]

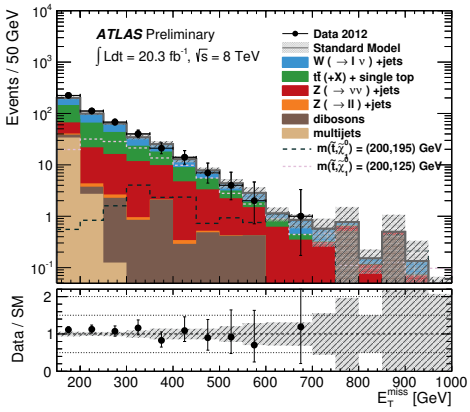

Figure 8: Measured $E_{\mathrm{T}}^{\mathrm{miss}}$ distribution for the charm-tagged selection compared to the SM predictions. The full signal selection is applied but the missing transverse energy is shown down to a value of 150 GeV. [7]

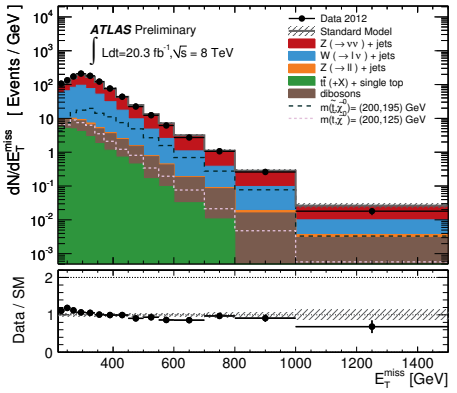

Figure 9: Measured $E_{\mathrm{T}}^{\mathrm{miss}}$ distribution for the monojet selection compared to the SM predictions. [7]

2.4 Direct stop production decaying to charm

The search [7] for direct top squark pair production in the decay channel to a charm quark and the lightest neutralino ($\tilde{t} \rightarrow c + \tilde{\chi}_1^0$) uses 20.3 fb^{-1} of pp collision data at $\sqrt{s} = 8$ TeV recorded by the ATLAS experiment at the LHC in 2012. In the compressed scenario with a mass difference $\Delta m = m_{\tilde{t}} - m_{\tilde{\chi}_1^0} < m_W + m_b$, the stop will dominantly decay via a loop process into a charm quark and a $\tilde{\chi}_1^0$ (LSP). The corresponding final state is characterised by the presence of two jets from the hadronization of the charm quarks and missing transverse momentum from the two undetected LSPs. However, given the relatively small mass difference Δm, both the transverse momenta of the two charm jets and the $E_{\mathrm{T}}^{\mathrm{miss}}$ are too low to extract this signal from the large multijet background. This study makes use of the presence of an initial-state radiation (ISR) jet to identify signal events. Figure 8 shows the $E_{\mathrm{T}}^{\mathrm{miss}}$ distribution for a moderate Δm where the charm jets receive a large boost from the ISR recoil to be detected. It is the first time at the LHC that charm tagging algorithms are used to enhance SUSY signal. Figure 9 shows the $E_{\mathrm{T}}^{\mathrm{miss}}$ distribution for the region in which stop and lightest neutralino are nearly degenerate in mass so that c-jets are too soft to be tagged. A monojet-like [9] analysis, where events are then characterised by a small number of jets, targets this region.

Good agreement is observed between the data and the SM predictions. The results are translated into new 95% CL exclusion limits on the stop and neutralino masses. Figure 10 shows the exclusion limits. A top squark mass of 200 GeV is excluded at 95% confidence level for $m_{\tilde{t}} - m_{\tilde{\chi}_1^0} < 85$ GeV. Top squark masses up to 230 GeV are excluded for a neutralino mass of 200 GeV. This extends significantly previous Tevatron results.

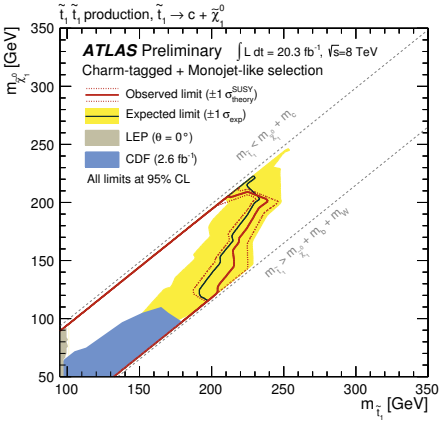

Figure 10: Exclusion plane at 95% CL. as a function of stop and neutralino masses. The observed (red line) and expected (black line) upper limits from this analysis are compared to previous results from Tevatron experiments, and from LEP experiments at CERN with squark mixing angle θ^0. [7]

3 Electroweak production

3.1 Direct slepton and chargino-pair production into two opposite-signed leptons

Searches for electroweak production of sleptons and charginos can produce final states with two oppositely-charged leptons (electrons or muons) and missing transverse momentum [10]. Direct production is targeted through three scenarii: pair-produced charged sleptons $q\bar{q} \to \tilde{\ell}^+\tilde{\ell}^-$, where each slepton decays to a lepton and an LSP $\tilde{\ell}^\pm \to \ell\tilde{\chi}_1^0$ (leading to different flavour $e^\pm\mu^\mp$), direct chargino-pair production $q\bar{q} \to \tilde{\chi}_1^+\tilde{\chi}_1^+$ where each chargino decays through $\tilde{\chi}_1^\pm \to (\tilde{\ell}^\pm\nu$ or $\ell^\pm\tilde{\nu}) \to \ell^\pm\nu\tilde{\chi}_1^0$, and an on- or off-shell W boson if the chargino decays as $\tilde{\chi}_1^\pm \to W^\pm\tilde{\chi}_1^0$, in case the latest chargino is the next-to-lightest SUSY particle (NLSP). This last analysis uses only the $e^\pm\mu^\mp$ channel because of the smaller background. For the three possibilities, no significant excesses are observed with respect to the prediction from Standard Model processes. Limits are set on the masses of the slepton and of the lightest chargino. Figures 11, 12 and 13 show the exclusion limits for each of the three analyses considered, using 20.3 fb^{-1} of pp collision data at $\sqrt{s} = 8$ TeV recorded by ATLAS.

3.2 Direct gaugino production into one lepton and two b-jets from a Higgs boson

A search for direct production of charginos $\tilde{\chi}_1^+$ and neutralinos $\tilde{\chi}_2^0$ exploits for the first time in electroweak SUSY searches at the LHC the presence of a Higgs boson in the decay chain [11]. The direct production of a chargino-neutralino pair $pp \to \tilde{\chi}_1^\pm\tilde{\chi}_2^0$ is followed by the chargino decay $\tilde{\chi}_1^\pm \to W^\pm(\to \ell^\pm\nu)\tilde{\chi}_1^0$ and the neutralino decay $\tilde{\chi}_2^0 \to h(\to b\bar{b})\tilde{\chi}_1^0$, where the $\tilde{\chi}_1^0$ is the LSP and $\tilde{\chi}_1^\pm$ and $\tilde{\chi}_2^0$ are assumed to be mass degenerate. The final-state signature contains one lepton (electron or muon), two jets and large missing transverse momentum. The jets are identified as originating from b-quarks (b-jets) consistent with a Higgs boson (BR($h \to b\bar{b}$) = 0.58). A large $E_{\mathrm{T}}^{\mathrm{miss}}$ cut helps removing the competing SM background. Figures 14 (15) show the di-jet mass m_{bb} spectrum for the signal regions sensitive to low (high) $\tilde{\chi}_1^\pm/\tilde{\chi}_2^0$ masses, using 20.3fb^{-1} of pp collision data at $\sqrt{s} = 8$ TeV recorded by ATLAS. No significant excess is observed with respect to the prediction from SM processes. Figure 16 displays 95% CL exclusion region obtained in the $m_{\tilde{\chi}_1^0}$–$m_{\tilde{\chi}_1^\pm}$ plane. Limits are set on the $\tilde{\chi}_1^\pm/\tilde{\chi}_1^0$mass such that for massless $\tilde{\chi}_1^0$, the ranges $125 < m_{\tilde{\chi}_1^\pm/\tilde{\chi}_1^0} < 141$ GeV and $166 < m_{\tilde{\chi}_1^\pm/\tilde{\chi}_1^0} < 287$ GeV are excluded at 95% CL, with an expected exclusion range of $225 < m_{\tilde{\chi}_1^\pm/\tilde{\chi}_1^0} < 235$ GeV.

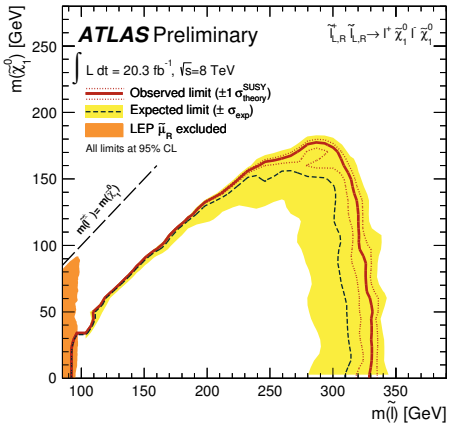

Figure 11: 95% CL exclusion limits for both right- and left handed (mass degenerate) selectron and smuon production in the $m_{\tilde{\chi}_1^0}$–$m_{\tilde{\ell}}$ plane. A common value for left and right-handed slepton masses between 90 GeV and 320 GeV is excluded at 95% confidence level for a massless neutralino. [10]

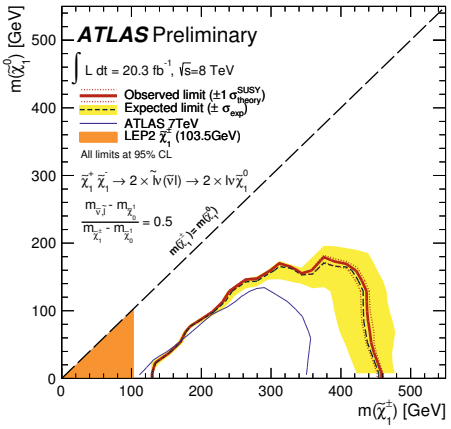

Figure 12: 95% CL exclusion limits for $\tilde{\chi}_1^+\tilde{\chi}_1^+$ pair production in the simplified model with sleptons and sneutrinos with $m_{\tilde{\ell}} = m_{\tilde{\nu}} = (m_{\tilde{\chi}_1^+} + m_{\tilde{\chi}_1^0})/2$. Chargino masses between 130 GeV and 450 GeV are excluded at 95% confidence level for a 20 GeV neutralino. [10]

Figure 13: Observed and expected 95% CLs upper limits of the cross-section as a function of $m_{\tilde{\chi}_1^+}$ for massless $\tilde{\chi}_1^0$ normalised to the simplified-model cross-section. The excluded cross-section is above the model cross-section by a factor 1.9 - 2.8 in the $\tilde{\chi}_1^\pm$ mass range 100 - 190 GeV and then degrades gradually to 4.7 when reaching $\tilde{\chi}_1^\pm$ mass of 250 GeV. Best sensitivity is obtained for the $(m_{\tilde{\chi}_1^\pm}, m_{\tilde{\chi}_1^0})$ = (100, 0) GeV mass point where $\sigma/\sigma_{\mathrm{SUSY}} = 1.8$. [10]

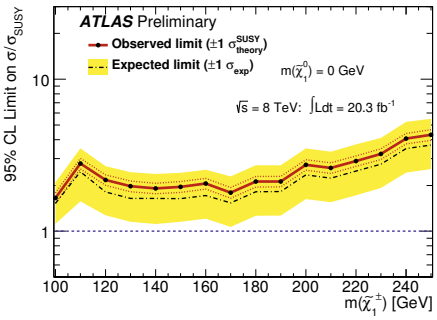

3.3 Three lepton exclusion limits

Figures 17 and 18 show the expected 95% CL limit contours for chargino and neutralino production in the three lepton analysis [12] performed using 20.7 fb^{-1} of pp collision data at $\sqrt{s} = 8$ TeV recorded by ATLAS. The former exhibits a very strong exclusion due to the 100% BR of sleptons to leptons. The exclusion in the decay via gauge bosons is limited due to the W and Z leptonic branching ratios.

4 Conclusion

No significant excess above expectations from the Standard Model has been observed in the searches of 3^{rd} generation squarks and electroweak production with ATLAS detector at LHC. Stringent limits

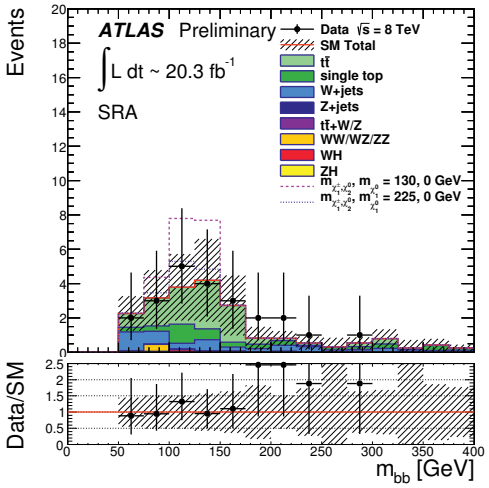

Figure 14: Distribution of m_{bb} for region SRA, sensitive to low $\tilde{\chi}_1^{\pm}/\tilde{\chi}_2^0$ masses. [11]

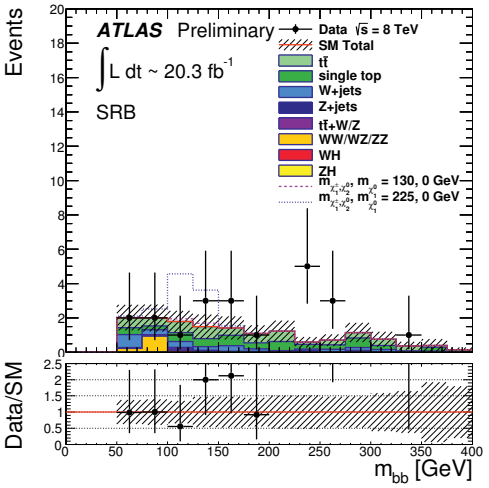

Figure 15: Distribution of m_{bb} for region SRB, sensitive to high $\tilde{\chi}_1^{\pm}/\tilde{\chi}_2^0$ masses. [11]

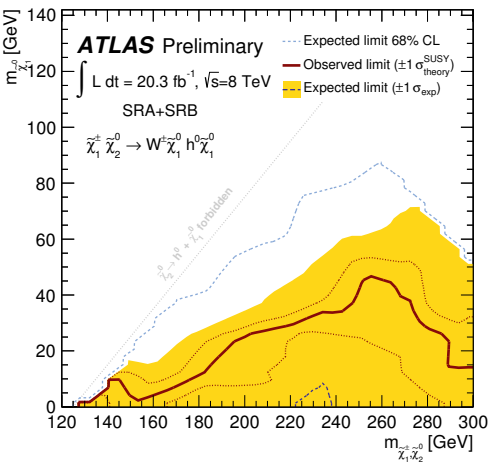

Figure 16: Exclusion limits in the $m_{\tilde{\chi}_1^{\pm}\tilde{\chi}_2^0}$–$m_{\tilde{\chi}_1^0}$ plane. The 68% CL expected exclusion limit is also shown. [11]

on sbottom, stop, gauginos and slepton masses have been set. Further studies, in particular the next run with data at $\sqrt{s} = 13$ TeV, will shed light on possible existence of superpartners.

References

[1] ATLAS Collaboration, JINST **3** S08003 (2008)

[2] ATLAS Collaboration, submitted to Journal of High Energy Physics, preprint `hep-ex/1308.2631` (2013)

[3] M. Cacciari, G. P. Salam, and G. Soyez, *The anti-kt jet clustering algorithm*, JHEP **04**063, `arXiv:0802.1189` (2008)

[4] D. Tovey, *On measuring the masses of pair-produced semi-invisibly decaying particles at hadron colliders*, JHEP **04** 034, `arXiv:0802.2879` (2008)

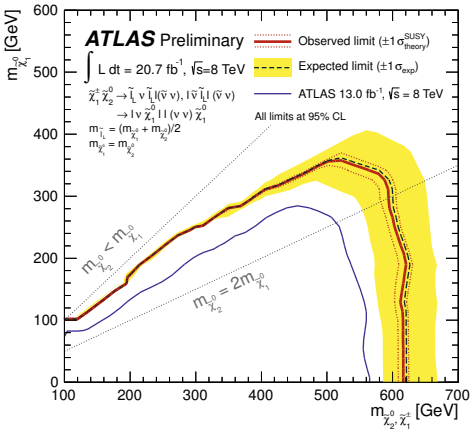

Figure 17: Observed and expected 95% CL limit contours for chargino and neutralino production in the simplified model scenario with decay via sleptons. [12]

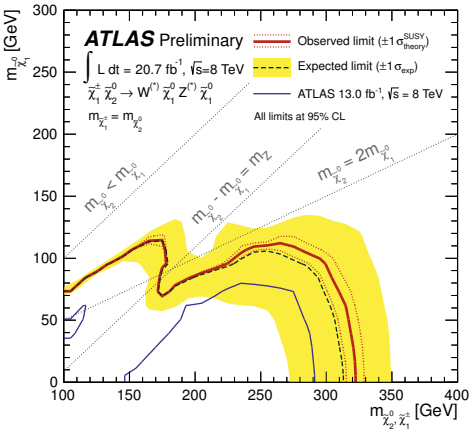

Figure 18: Observed and expected 95% CL limit contours for chargino and neutralino production in the simplified model scenario with decay via bosons. [12]

[5] ATLAS Collaboration, ATLAS-CONF-2013-061, https://cds.cern.ch/record/1557778 (2013)
[6] ATLAS Collaboration, ATLAS-CONF-2013-065, https://cds.cern.ch/record/1562840 (2013)
[7] ATLAS Collaboration, ATLAS-CONF-2013-068, https://cds.cern.ch/record/1562880 (2013)
[8] ATLAS Collaboration, ATLAS-CONF-2013-048, https://cdsweb.cern.ch/record/154756 (2013)
[9] ATLAS Collaboration , ATLAS-CONF-2012-147, https://cdsweb.cern.ch/record/1493486 (2012)
[10] ATLAS Collaboration, ATLAS-CONF-2013-049, https://cdsweb.cern.ch/record/1547565 (2013)
[11] ATLAS Collaboration, ATLAS-CONF-2013-093, https://cdsweb.cern.ch/record/1595756 (2013)
[12] ATLAS Collaboration, ATLAS-CONF-2013-35, https://cdsweb.cern.ch/record/1532426 (2013)